

## Supplementary Material

### **Tunability of electronic properties in 2D MoS<sub>2</sub>/α-tellurene/WS<sub>2</sub> heterotrilayer via biaxial strain and electric field**

Wenli Zhang,<sup>a</sup> Zhuang Ma,<sup>b</sup> Jing Wang,<sup>a</sup> Bin Shao<sup>\*ac</sup> and Xu Zuo<sup>\*ade</sup>

<sup>a</sup>*College of Electronic Information and Optical Engineering, Nankai University, Tianjin 300350, China*

<sup>b</sup>*School of Physics and Telecommunication Engineering, Zhoukou Normal University, Zhoukou 466001,  
China*

<sup>c</sup>*Tianjin Key Laboratory of Optoelectronic Sensor and Sensing Network Technology, Nankai University,  
Tianjin 300350, China*

<sup>d</sup>*Key Laboratory of Photoelectronic Thin Film Devices and Technology of Tianjin, Tianjin 300350, China*

<sup>e</sup>*Engineering Research Center of Thin Film Optoelectronics Technology, Ministry of Education, Tianjin,  
300350, China*

**\*Correspondence:**

Bin Shao

bshao@nankai.edu.cn

Xu Zuo

xzuo@nankai.edu.cn

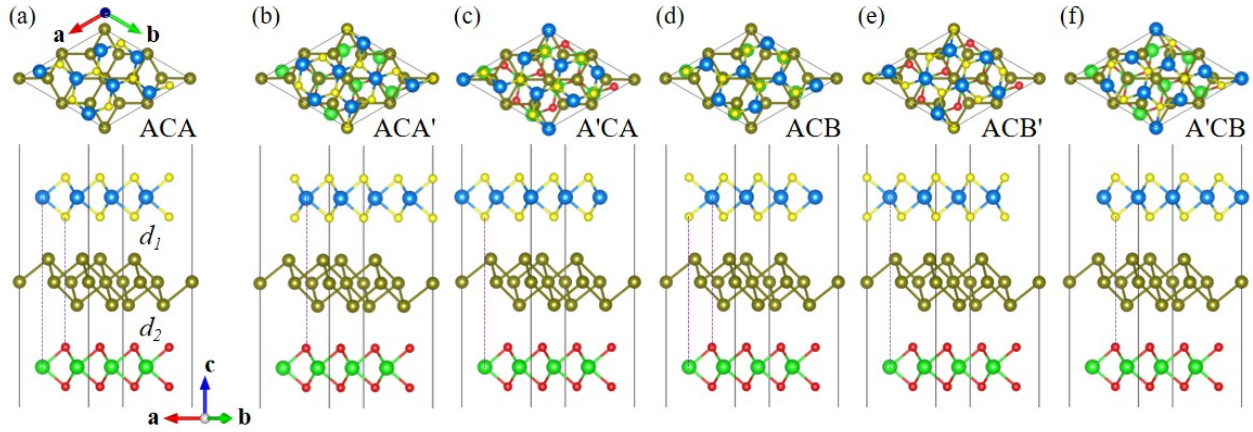


**Fig. S1.** (a-f) Top and side views of  $\text{MoS}_2/\alpha\text{-Te}/\text{WS}_2$  heterotrilityer with six different stacking patterns.

**Table S1.** The interlayer distance ( $d$ ) of  $\text{MoS}_2/\alpha\text{-Te}/\text{WS}_2$  heterotrilityer under different stacking patterns and the relative energy ( $\Delta E$ ) with the ACA configuration as a reference.

	ACA	ACA'	A'CA	ACB	ACB'	A'CB
$d_1$ (Å)	3.352	3.375	3.353	3.352	3.362	3.356
$d_2$ (Å)	3.347	3.337	3.356	3.356	3.338	3.341
$\Delta E$ (meV)	0	-8.72	3.27	3.01	-7.59	1.33

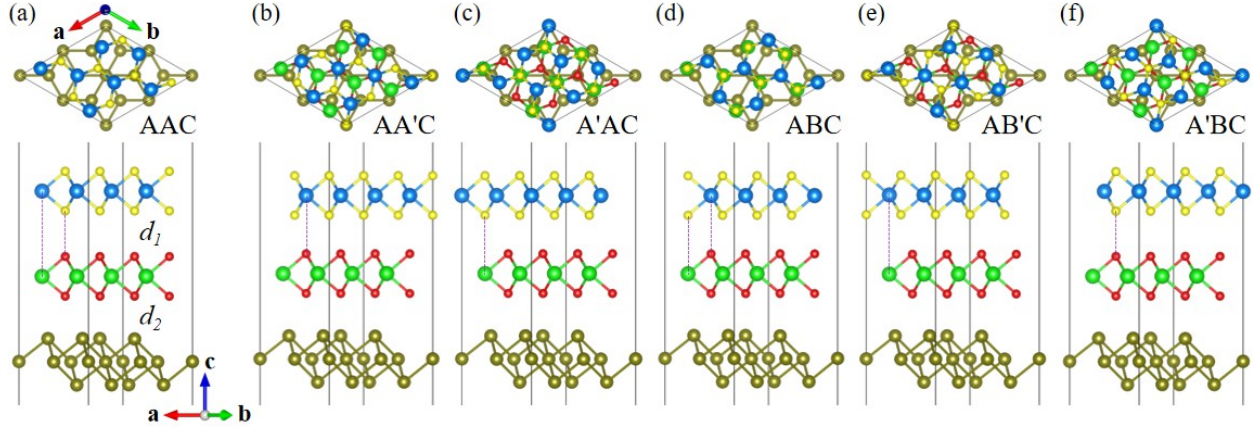


**Fig. S2.** (a-f) Top and side views of MoS<sub>2</sub>/WS<sub>2</sub>/α-Te heterotrilinear with six different stacking patterns.

**Table S2.** The interlayer distance ( $d$ ) of MoS<sub>2</sub>/WS<sub>2</sub>/α-Te heterotrilinear under different stacking patterns and the relative energy ( $\Delta E$ ) with the AAC configuration as a reference.

	AAC	AA'C	A'AC	ABC	AB'C	A'BC
$d_1$ (Å)	3.607	3.050	3.045	3.045	3.126	3.573
$d_2$ (Å)	3.349	3.350	3.353	3.314	3.317	3.340
$\Delta E$ (meV)	0	-457.24	-469.76	-471.51	-363.90	-21.61

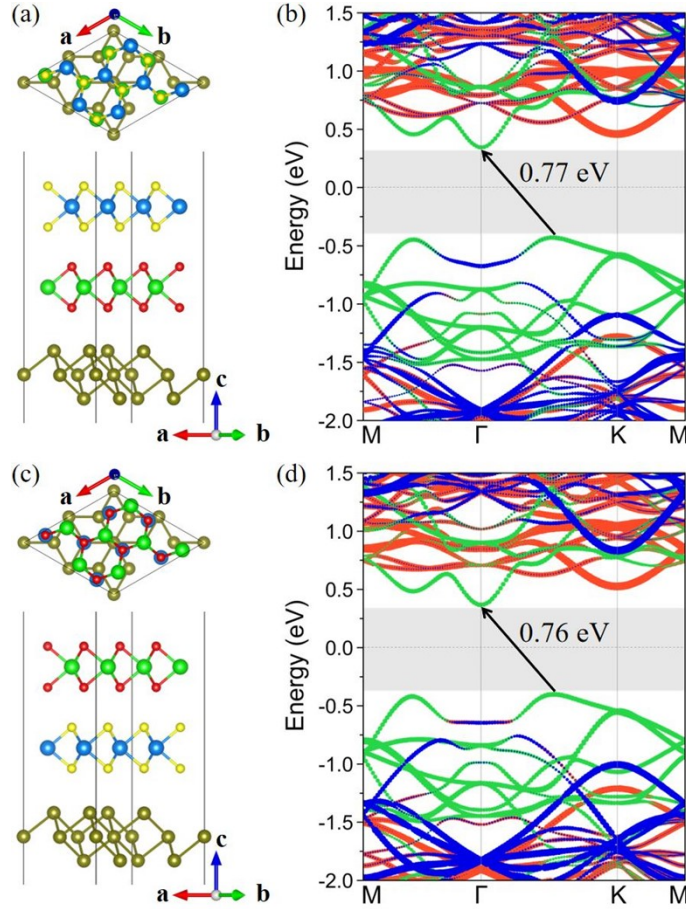


**Fig. S3.** Top and side views of (a) MoS<sub>2</sub>/WS<sub>2</sub>/α-Te and (c) WS<sub>2</sub>/MoS<sub>2</sub>/α-Te heterotrilayers. Atomic projected band structures of (b) MoS<sub>2</sub>/WS<sub>2</sub>/α-Te and (d) WS<sub>2</sub>/MoS<sub>2</sub>/α-Te heterotrilayers. The red, green, and blue solid lines represent the contributions of MoS<sub>2</sub>, α-Te, and WS<sub>2</sub>, respectively, with the radius of the data points reflecting the proportion of each component.

As representative members of the TMD family, MoS<sub>2</sub> and WS<sub>2</sub> share identical lattice constants and similar electronic properties. As shown in Fig. S3, the stacking order of these two monolayers on the α-Te substrate has a negligible impact on the overall band structure. Consequently, we selected only one of them as the focus of our study.

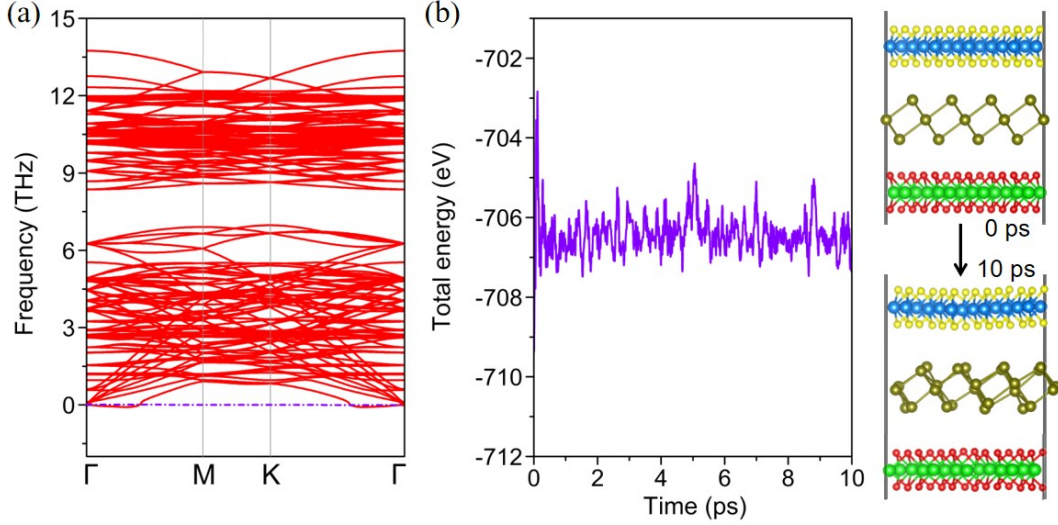


**Fig. S4.** (a) Phonon spectra in the whole Brillouin zone of MoS<sub>2</sub>/α-Te/WS<sub>2</sub> heterotrilinear. (b) The total energy as a function of time during AIMD simulations of MoS<sub>2</sub>/α-Te/WS<sub>2</sub> heterotrilinear at 300 K.

We have confirmed the dynamic and thermodynamic stability of the MoS<sub>2</sub>/α-Te/WS<sub>2</sub> heterotrilinear through phonon spectra and *ab initio* molecular dynamics (AIMD) simulations. Firstly, phonon dispersion curves are calculated using a  $2 \times 2 \times 1$  supercell through the density functional perturbation theory (DFPT) method, as shown in Fig. S4(a). The dynamic stability of the heterostructure can be verified by the absence of imaginary frequencies in the phonon spectra across the whole Brillouin zone. It is worth noting that a finite supercell used for phonon calculations may introduce numerical inaccuracies, with a minor imaginary frequency of approximately 0.08 THz emerging at the  $\Gamma$  point. However, this phenomenon is also observed in numerous 2D systems<sup>1-3</sup> and is associated with the acoustic properties of a real freestanding system, corresponding to a collective vibration mode with a long wavelength approaching infinity. While ripples may be induced, their impact on the overall stability of the structure is expected to be negligible. Subsequently, as illustrated in Fig. S4(b), the AIMD simulations conducted at 300 K reveal minimal fluctuations in the total energy of the heterotrilinear. Throughout the simulation duration, the atomic structure exhibits only slight displacements from the equilibrium position without any noticeable structural damage, thereby indicating the thermodynamic stability of the heterotrilinear.

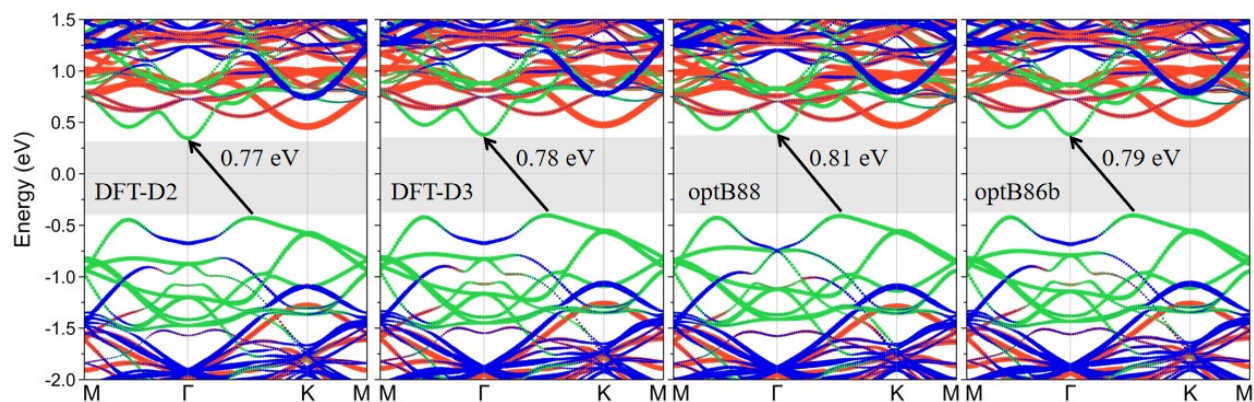


**Fig. S5.** Projected band structures of MoS<sub>2</sub>/WS<sub>2</sub>/ $\alpha$ -Te heterotrilinear with different vdW corrections. The red, green, and blue solid lines represent the contributions of MoS<sub>2</sub>,  $\alpha$ -Te, and WS<sub>2</sub>, respectively, with the radius of the data points reflecting the proportion of each component.

The interlayer vdW interaction in 2D materials is a non-bonding interaction. Compared with chemical bonds, this weaker interaction allows for the arbitrary stacking of 2D materials, facilitating the formation of vdW heterostructures and Moiré superlattices, leading to various novel physical, chemical, and mechanical properties. Generally speaking, there are typically two approaches to describe the weak interlayer vdW interaction. One involves incorporating a dispersion correction term based on the PBE function, using either the DFT-D2 or DFT-D3 methods. The other involves modifying the exchange-correlation term to account for vdW corrections, such as the optB88-vdW and optB86b-vdW methods. As shown in Fig. S5, all of these correction methods can reproduce similar electronic properties. Therefore, we chose to employ the more commonly used DFT-D2 method to correct the vdW interaction.

## References

- [1] Y. Shao, M. Shao, Y. Kawazoe, X. Shi and H. Pan, *J. Mater. Chem. A*, 2018, **6**, 10226–10232.
- [2] Z. Ma, P. Huang, J. Li, P. Zhang, J. Zheng, W. Xiong, F. Wang and X. Zhang, *Npj Comput. Mater.*, 2022, **8**, 51.
- [3] H. Zhang, Y. Li, J. Hou, A. Du and Z. Chen, *Nano Lett.*, 2016, **16**, 6124–6129.